Low Temperature Physics/Fizika Nizkikh Temperatur, 2016, v. 42, No. 6, pp. 567–572

Density domains of a photo-excited electron gas on liquid helium

Yu.P. Monarkha

B. Verkin Institute for Low Temperature Physics and Engineering of the National Academy of Sciences of Ukraine
47 Prospekt Nauky, Kharkiv 61103, Ukraine
E-mail: monarkha@ilt.kharkov.ua

Received February 17, 2016, published online April 25, 2016

The Coulombic effect on the stability range of the photo-excited electron gas on liquid helium is shown to favor formation of domains of different densities. Domains appear to eliminate or greatly reduce regions with negative conductivity. An analysis of the density domain structure allows explaining remarkable observations reported recently for the photo-excited electron gas.

PACS: **73.40.–c** Electronic transport in interface structures;
73.20.–r Electron states at surfaces and interfaces;
78.67.–n Optical properties of low-dimensional, mesoscopic, and nanoscale materials and structures;
78.70.Gq Microwave and radio-frequency interactions;
73.25.+i Surface conductivity and carrier phenomena.

Keywords: Coulombic effect, liquid helium, photo-excited electron gas.

Properties of a 2D electron gas exposed to a perpendicular magnetic field B and irradiated with microwaves (MW) recently became a subject of intense studies because of new interesting discoveries. In GaAs/AlGaAs heterostructures, novel $1/B$-periodic MW-induced resistance oscillations (MIRO) [1] and zero-resistance states (ZRS) [2,3] were observed, when the MW frequency ω was larger than the cyclotron frequency $\omega_c = eB/Mc$. The ZRS appears in the vicinity of a resistance minimum near $\omega/\omega_c = m + 1/4$, where m is an integer. These observations have attracted much interest, and a number of theoretical mechanisms were proposed to explain MIRO [4,5,6,7] and ZRS [8,9].

Similar $1/B$-periodic oscillations of the dc magnetoconductivity σ_{xx} and the ZRS were observed in the 2D electron system formed on the surface of liquid helium [10,11], when the system was tuned to the resonance with the MW frequency, $\Delta_2 - \Delta_1 = \hbar\omega$ (here Δ_l is the energy of surface subbands, $l = 1, 2, ...$). Therefore, the period of these oscillations was actually governed by the ratio $\omega_{2,1}/\omega_c$ where $\omega_{2,1} = (\Delta_2 - \Delta_1)/\hbar$. The theory of this effect [12] is based on nonequilibrium filling of the second surface subband, $N_2 > N_1 \exp(-\hbar\omega_{2,1}/T_e)$, which triggers intersubband electron scattering against or along the in-plane dc electric field E_{dc} depending on the sign of $\omega_{2,1}/\omega_c - m$. At strong enough power, the sign-changing contribution to the effective collision frequency can make $\sigma_{xx} < 0$, which by itself suffices to explain the existence of the ZRS [8]. For surface electrons (SEs) on liquid helium, minima of σ_{xx} are not strictly fixed to the condition $\omega_{2,1}/\omega_c = m + 1/4$. Their positions depend on the strength of Coulomb interaction between electrons and on the number m [13,14].

A state of an electron system with $\sigma_{xx} < 0$ is unstable [8], and usually a certain local current density j_0 is necessary to reach the stable state where $\sigma_{xx}(j_0) = 0$. This predicts the existence of current domains, where electrons move in opposite directions [8]. Such a model of the ZRS is well applicable for semiconductor electrons. SEs on liquid helium represent a highly correlated system, where the average Coulomb interaction potential energy per an electron U_C is much larger than the average kinetic energy. In such a system, current domains are unlikely due to the strong mutual friction of currents in the domain wall. Therefore, the internal structure of the ZRS of SEs on liquid helium is under the question. Experimental observation of an ultra-strong photovoltaic effect [15] which emerges in the regime $\sigma_{xx} \to 0$ gives an important insight into this problem. This effect is characterized by a strong displacement of electrons against the confining force of Corbino electrodes placed below the liquid helium surface (electrons are displaced from the center of the plane towards the edge). Remarkably, the redistributed charge exhibits spontaneously generated oscillations in the audio-frequency range [16].

Recently a striking example of irradiation-induced self-organization was observed [17] in a coupled system of two electron gases of different densities. The 2D electron gases

were formed on the surface of liquid ^{4}He above the central Corbino electrode (with density n_e) and above the guard-ring electrode (with density n_g). At a fixed total number of electrons N_e, the ratio n_e/n_g was varied by changing the potential V_g applied to the guard electrode. In the presence of resonant MW radiation, under the magnetic field fixed to the ZRS condition, $\omega_{2,1}/\omega_c(B) = 6.25$, the inner 2D electron gas enters an incompressible state with an electron density $n_e = n_c \simeq 3.4\cdot 10^6\,\mathrm{cm}^{-2}$ independent of N_e and of the potential applied to the guard electrode for a wide range of parameters.

Surprisingly new discoveries reported for SEs in the regime of vanishing σ_{xx} (the photovoltaic effect, self-generated oscillations, and the incompressible state) have no convincing explanations and require additional theoretical studies of the nature of the ZRS in a highly correlated electron system. In this work, we report results of theoretical study of Coulombic effects on the stability range of the electron system under conditions of experiments [15–17]. We found that for a magnetic field fixed near a magnetoconductivity minimum, usually there are two electron densities n_H and n_L (here $n_H > n_L$) which restrict the unstable region where $\sigma_{xx} < 0$. Values of n_H and n_L are determined only by B and the MW power. Such an unusual dependence of σ_{xx} on electron density allows us to formulate the density domain structure of the ZRS of SEs on liquid helium which explains recent observations [15–17].

It is instructive to consider the dependence of $\sigma_{xx}(B)$ in the vicinity of a conductivity minimum using the microscopic mechanism of magneto-oscillations [13] applicable for electrons with $U_C \gg T$. At low temperatures, the momentum relaxation of SEs is determined by electron interaction with capillary wave quanta (ripplons). New features of the theory follow from the structure of the average probability of intersubband scattering from $l = 2$ to $l = 1$ accompanied by the momentum exchange $\hbar\mathbf{q}$ due to ripplon destruction and creation $\nu_{2\to1}(\mathbf{q})$, which depends on the average electron velocity $\mathbf{V}$. Under the conditions $V_y \simeq -V_H$ and $|V_x| \ll V_H$ (here $V_H = cE_{dc}/B$) this quantity is found as [13]

$$\nu_{2\to1}(\mathbf{q}, V_H) = 2p_{2,1}^2(q)\, S_{2,1}\left(q, \omega_{2,1} + q_y V_H\right), \qquad (1)$$

where $p_{2,1}^2(q)$ is defined by electron–ripplon coupling, and $S_{2,1}(q,\Omega)$ is a generalization of the dynamic structure factor of the 2D electron liquid which takes into account that Landau levels have different collision broadening Γ_l for different subbands. The Eq. (1) has sharp maxima at $\omega_{2,1} + q_y V_H \to m\omega_c$ caused by the Landau level matching $(m = n' - n)$.

Electron–ripplon scattering is quasi-elastic because typical ripplon energies $\hbar\omega_q \ll \Gamma_1$ for $q \lesssim 1/L_B$, where $L_B^2 = \hbar c/eB$. In Eq. (1), the correction $q_y V_H$ originates from $eE_{dc}(X' - X) = \hbar q_y V_H$. When evaluating the decay rate of the excited subband, $q_y V_H$ can be neglected. Therefore, $S_{2,1}(q, \omega_{2,1})$ and $\nu_{2\to1}(\mathbf{q})$ have sharp maxima at $\omega_{2,1} \simeq m\omega_c$. For the Gaussian shape of the Landau level density of states [18], the maxima are also proportional to a Gaussian $G(w) = \exp(-w^2/\tilde{\gamma}^2)/\sqrt{\pi}\tilde{\gamma}$, where [13]

$$w = \frac{\omega_{2,1}}{\omega_c} - m - \frac{\Gamma_2^2}{4T_e\hbar\omega_c} - x_q\frac{\Gamma_C^2}{4T_e\hbar\omega_c}, \qquad (2)$$

$$\tilde{\gamma} = \frac{1}{\hbar\omega_c}\sqrt{\frac{\Gamma_1^2 + \Gamma_2^2}{2} + x_q\Gamma_C^2}, \quad x_q = \frac{q^2L_B^2}{2}, \qquad (3)$$

T_e is the electron temperature, and $\sqrt{x_q}\Gamma_C$ is an additional broadening of the dynamic structure factor induced by Coulomb interaction. Considering the fluctuational electric field E_f [19], acting on an electron, as a quasi-uniform field yields $\Gamma_C = \sqrt{2}E_f^{(0)}L_B$ [20], where $E_f^{(0)} \simeq 3\sqrt{T_e}n_s^{3/4}$ and n_s is the SE density. In Eq. (2), the third term is very small because $\Gamma_l \ll T_e$ and $\Gamma_l \ll \hbar\omega_c$. The last term can be substantial at high electron densities or at large level matching numbers m when the average value of the parameter x_q increases. For conditions of experiments [15–17], it is also small.

Intersubband scattering $2 \to 1$ is accompanied by the momentum exchange $\hbar\mathbf{q}$, whose average value can be obtained expanding Eq. (1) in $q_y V_H$. Thus, the corresponding contribution into the electron momentum relaxation rate is proportional to the derivative of the Gaussian $G'(w) = -2\tilde{\gamma}^{-2}wG(w)$, and it changes sign at $\omega_{2,1}/\omega_c = m$. This determines the shape of magnetoconductivity oscillations and allows to estimate positions of minima. If we neglect overlapping of the sign-changing terms in the sum over the all m, then positions of minima are given by

$$\omega_{2,1}/\omega_c - m = \tilde{\gamma}/\sqrt{2} + x_q\frac{\Gamma_C^2}{4T_e\hbar\omega_c}. \qquad (4)$$

The deviation from the level matching point increases monotonically with electron density due to the Coulomb broadening Γ_C entering also $\tilde{\gamma}$. At large m, when the sign-changing terms become strongly overlapping, the positions of minima are asymptotically given by

$$\frac{\omega_{2,1}}{\omega_c} - m = \frac{1}{4} + x_q\frac{\Gamma_C^2}{4T_e\hbar\omega_c}, \qquad (5)$$

where we can use the estimation $x_q \sim m$.

The analysis given above indicates that a position of a conductivity minimum generally depends strongly on n_s: an increase of n_s lifts up the position of the minimum and shifts it right along the $\omega_{2,1}/\omega_c$-axis, as follows from Eqs. (4) and (5). This means that changing electron density itself can eliminate the unstable state with $\sigma_{xx} < 0$. It should be noted that experimental data show somewhat larger shifts of σ_{xx} minima than those given by the theory because it disregards heating of SEs. Still, the theory describes well the nontrivial dependence of conductivity

extrema on n_s and m [14]. Therefore, we shall use the approximation $T_e = T$ to obtain stability range of the electron system under intersubband excitation keeping in mind that decay heating of SEs can affect our estimations.

In the region of interest, the results of numerical evaluations are shown in Fig. 1. It demonstrates the evolution of the conductivity minimum with decreasing n_s from $7.25\cdot10^6\,\mathrm{cm}^{-2}$ to $5\cdot10^6\,\mathrm{cm}^{-2}$ for a fixed MW power. The vertical line indicates a fixed magnetic field chosen for our analysis. The cross-points of this line with curves $\sigma_{xx}(\omega_{2,1}/\omega_c)$ shown by circles indicate values of σ_{xx} for the given B and n_s. The open circle indicates the first appearance of the ZRS. Any shift of the vertical line (chosen value of $\omega_{2,1}/\omega_c$) left or right eliminates this ZRS.

For a lower electron density $n_s = 6\cdot10^6\,\mathrm{cm}^{-2}$, we have an unstable state with $\sigma_{xx} < 0$ shown by the lower black circle. With lowering n_s curves $\sigma_{xx}(\omega_{2,1}/\omega_c)$ shift left in accordance with Eqs. (4) and (5). Eventually, at $n_s = 5.5\cdot10^6\,\mathrm{cm}^{-2}$ the corresponding curve $\sigma_{xx}(\omega_{2,1}/\omega_c)$, again crosses the vertical line at the point shown by the open circle which indicates the ZRS. Further reduction in n_s leads to a state with $\sigma_{xx} > 0$, as shown by the curve calculated for $n_s = 5\cdot10^6\,\mathrm{cm}^{-2}$ and by the higher black circle. Thus, for a fixed magnetic field, the instability ($\sigma_{xx} < 0$) appears inside a certain region restricted by two densities (higher n_H and lower n_L). At $n_s = n_H$, or at $n_s = n_L$ the system is in the ZRS.

The length of the unstable region $n_H - n_L$ depends strongly on the position of the vertical line with regard to the ZRS appeared for the solid curve of Fig. 1. For example, consider the conditions illustrated in Fig. 2. Here we chose two magnetic fields B_1 and B_2 indicated by vertical lines which are located at the left and right sides with regard to the minima of the solid curve. The crossing points

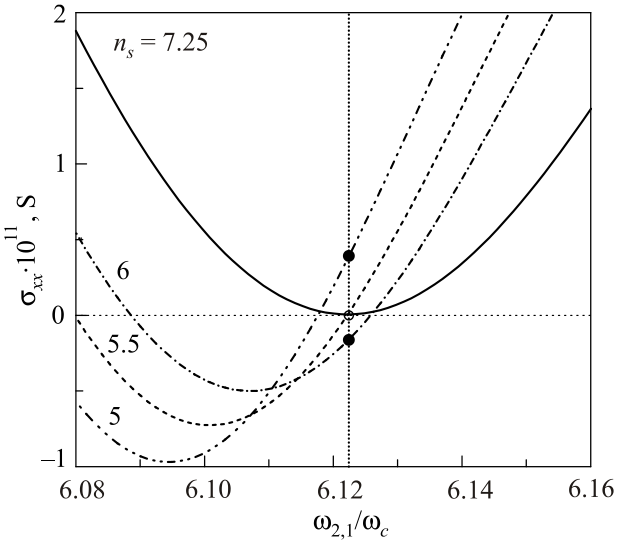

Fig. 1. Magnetoconductivity in a dc electric field E_{dc} vs $\omega_{2,1}/\omega_c$ calculated for $T = 0.3$ K (liquid ^{4}He) and four n_s. Values of n_s are shown in units of 10^6 cm^{-2}.

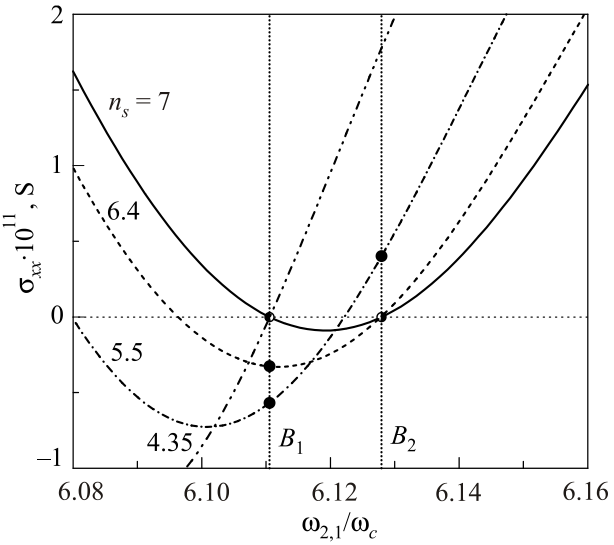

Fig. 2. Magnetoconductivity in a dc electric field E_{dc} vs $\omega_{2,1}/\omega_c$ calculated for four n_s. Values of n_s are shown in units of 10^6 cm^{-2}.

of the vertical lines with the solid curve give two ZRS which appear first when decreasing n_s. One can see that the range of states with $\sigma_{xx} < 0$ strongly differs for B_1 and B_2. For the right vertical line, it shrinks $n_H - n_L \simeq 0.6\cdot10^6\,\mathrm{cm}^{-2}$ as indicated by the dashed curve. For intermediate densities, the negative values of σ_{xx} are very close to zero, therefore, we didn't show a corresponding curve in this figure. To the contrary, for the left vertical line, we found a substantially larger instability range $n_H - n_L \simeq 1.5\cdot10^6\,\mathrm{cm}^{-2}$. Obviously, n_L can be reduced very much by shifting the vertical line left. Thus, fixing B and MW power defines two distinct values of electron density n_H and n_L where the 2D electron system enters the ZRS. For intermediate densities $n_L < n_s < n_H$, the system is unstable.

A negative σ_{xx} means that any density fluctuation δn_s (positive or negative) diffusively grows. The density of growing regions is limited by the conditions: $n_s + \delta n_s = n_H$ and $n_s + \delta n_s = n_L$. Therefore, the electron system with $n_L < n_s < n_H$ eventually will be separated into fractions (domains) with different densities n_H and n_L. For a Corbino geometry, the simplest stable pattern of the density distribution with a domain wall is shown in Fig. 3. Two arrows indicate that in different domains near the domain wall (dashed circle) local currents flow in the same direction in contrast with the case of current domains. The position of the domain wall (the areas S_H and S_L) corresponding to the initial density n_s is determined by the rule:

$$\frac{S_H}{S_L} = \frac{n_s - n_L}{n_H - n_s}. \qquad (6)$$

We assume that the direction of the charge displacement caused by negative conductivity should be opposite

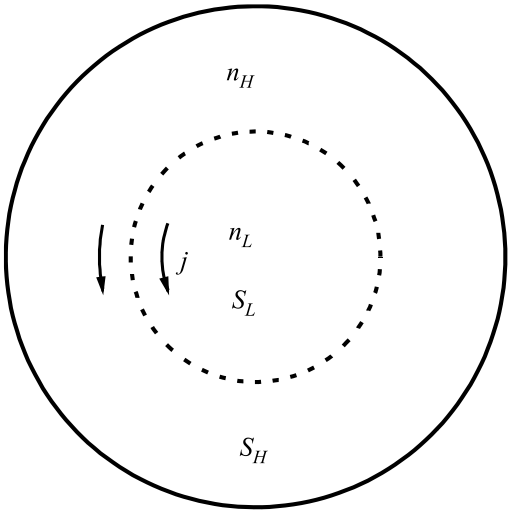

Fig. 3. The pattern of the density distribution with a domain wall for the Corbino geometry.

to the direction of the confining force of Corbino electrodes acting on SEs.

For a sharp domain wall, one can see that the separation of charges shown in Fig. 3 is stable until the resonant MW excitation keeps $\sigma_{xx} = 0$ in the domains. Assume some electrons by chance have moved from the area S_L to the area S_H. This makes $\sigma_{xx} > 0$ in both areas and the same amount of electrons will return back due to the inner electric field induced by charge separation. In a contrary case, when some electrons have moved from the area S_H to the area S_L, the magnetoconductivity in both domains became negative, and the same amount of electrons will return back moving in an uphill direction with regard to the local dc electric field. Therefore, under the condition of Eq. (6) the domain structure is in a dynamic equilibrium.

Formation of the domain structure caused by negative conductivity effects explains electron displacement towards the edge observed under resonant MW radiation [15]. According to our estimations the displaced fraction of electrons can be of the order of N_e which agrees with observations. In Ref. 15, the initial electron density (in the dark) was about $1.4 \cdot 10^6\,\mathrm{cm}^{-2}$ which is smaller than the value of the lower critical density n_L defined in Figs. 1 and 2. It should be noted that the calculations didn't take into account electron heating. For heated electrons, according to Eqs. (2) and (3), the same many-electron effect is produced by an electron density lower by the factor $(T/T_e)^{2/3}$ than it is for $T_e = T$. Assuming $T_e \approx 2$ K, we obtain the factor 0.2 which makes n_L less than the density used in the experiment [15].

Regarding self-generated oscillations observed in Ref. 16, first we note that the frequency of interior magnetoplasmons has a gap ω_c, and they cannot be a reason for audio-frequency oscillations. SEs on liquid helium have well-defined audio-frequency excitations: edge magnetoplasmons (EMP) [21,22] and inter-edge magnetoplasmons (IEMP) [23]. They are localized near the edge of a 2D electron system (EMP) or near internal boundary of two contacting regions with different densities (IEMP). Under a strong magnetic field, the spectrum of the IEMP is gapless, and its frequency decreases with B [24]

$$\omega_{IEMP} = 2q_y \left(\sigma_{yx}^H - \sigma_{yx}^L\right)\left(\ln\frac{1}{|q_y|b} + C\right), \qquad (7)$$

where $\sigma_{yx}^{H/L} \sim n_{H/L}/B$, the constant C depends on details of the density profile, b is the width of the transition layer, and q_y is the wavevector component along the boundary. If the inter-edge profile for the domain structure of Fig. 3 is sufficiently smooth, a negative dc conductivity can be ascribed to a narrow strip of the domain wall. It is quite obvious that this leads to a negative damping and to self-generation of the IEMP. The same argument is applicable to the EMP if the net conductivity within the edge profile is negative. Thus, experimental observation of self-generated audio-frequency oscillations [16] can be considered as a convincing evidence for negative conductivity coexisting with the ZRS of surrounding domains.

The appearance of two critical electron densities n_H and n_L restricting the instability range provides also an insight into the nature of the incompressible state observed for the system of two coupled 2D electron gases [17]. In this experiment, density domains were created artificially by applying different potentials to the guard (V_g) and central (V_e) electrodes of Corbino geometry. SEs were redistributed between these domains with areal densities n_g and n_e by varying V_g, so that at large V_g nearly all SEs were located above the guard-ring electrode ($n_g = N_e/S_g$, $n_e = 0$). In the opposite limit, SEs were concentrated

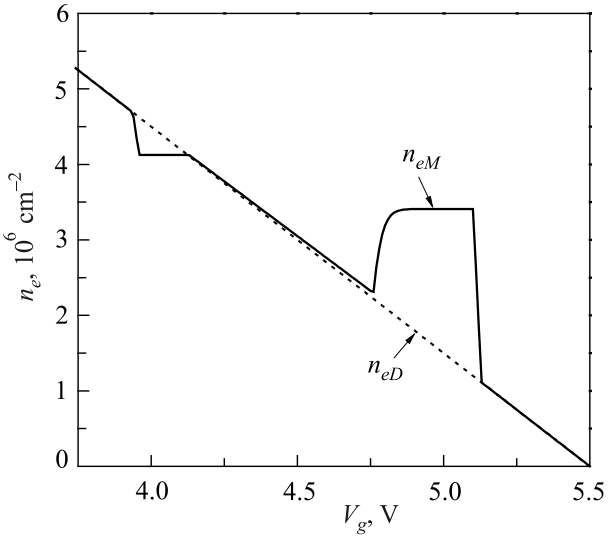

Fig. 4. A schematic plot showing how, typically, the electron density, n_e, varies with the guard voltage, V_g, in the experiment [17]: the dark case (dashed), irradiated SEs (solid).

above the central electrode: $n_g = 0$ and $n_e = N_e/S_e$. Here S_e and S_g are the areas of the central and guard electrodes respectively. The experimental dependence of $n_e(V_g)$ is shown schematically in Fig. 4. In the dark case (dashed line), electron compressibility defined as [17] $\chi = -dn_e/dV_g$ is nearly constant. Under MW radiation the dependence $n_e(V_g)$ changes drastically, as shown by the solid line marked n_{eM}. Below 5.13 V there is a sharp (nearly vertical) increase of n_{eM} up to a value $n_c \simeq 3.4\cdot10^6\,\mathrm{cm}^{-2}$. Then, there is a plateau with $\chi = 0$. Remarkably, in the range $4.75\ \mathrm{V} < V_g < 4.9\ \mathrm{V}$, the system exhibits a negative (!) compressibility: $\chi < 0$. At lower V_g, the $n_{eM}(V_g)$ returns to the dependence observed for the dark case.

The negative compressibility observed means that the 2D electron gas squeezes when we apply a potential to stretch it, and the gas expands when we apply a potential to compress it. This agrees with our understanding of negative conductivity effects. It should be noted that already from the existence of regions with $\sigma_{xx} < 0$ $(\chi < 0)$ and $\sigma_{xx} > 0$ $(\chi > 0)$ it follows that there should be at least one incompressible state in between them. The puzzling thing is that the incompressible state is observed in a quite broad region of V_g. Taking into account the results obtained here, we can expect anomalies on the dependence $n_{eM}(V_g)$ near n_H and n_L. Then, the plateau value n_c of Fig. 4 can be naturally ascribed to n_H, while the density to which the solid line falls down at $V_g \simeq 5.13$ V can be ascribed to n_L (note that the later density point is practically independent of N_e). Thus, we have $n_H \simeq 3.4\cdot10^6\,\mathrm{cm}^{-2}$ and $n_L \simeq 1.2\cdot10^6\,\mathrm{cm}^{-2}$. The small upper plateau formed at $V_g \sim 4$ V is close to the condition $n_g = n_L$.

To explain stability of the state with $n_e = n_H = n_c$ first we note that for n_e a bit lower than n_c, usually the both densities n_e and n_g enter the unstable region (n_g is somewhat larger than n_L). Therefore, for electrons moving against the confining force, domains with densities n_H (center) and n_L (edge) should appear to form the ZRS, as illustrated in Fig. 5. The radius of the central domain R_H is usually larger than the radius of the central electrode R_d. Therefore, the average density above the central electrode does not change with varying N_e. The density distribution shown in Fig. 5 is quite stable, and it should not change much with varying V_g. Assume that an electron somehow is displaced from the center to the edge domain. Then, the both regions enter the regime $\sigma_{xx} < 0$, and an electron will move in the uphill direction with regard to the total force **F** back to restore the ZRS, as shown in Fig. 5. The opposite displacement of an electron makes $\sigma_{xx} > 0$ and an electron will move back. Thus, redistribution of electrons between domains is locked out.

According to Eqs. (2) and (3) the Coulombic effect increases with m. Therefore, at larger m the n_H should be lower, which also agrees with observations [17].

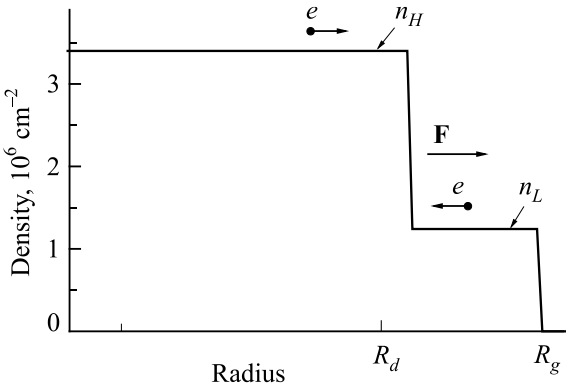

Fig. 5. The density domain structure proposed to explain the incompressible state observed in the experiment [17].

In summary, we have investigated theoretically the influence of Coulomb interaction acting between electrons on the stability range of the photo-excited electron gas on liquid helium. The analysis given here allows us to conclude that the zero resistance state of SEs is formed of two domains of different densities. This conception gives explanations for the photovoltaic effect [15], self-generated audio-frequency oscillations [16], and an incompressible state [17] recently observed in experiments.

1. M.A. Zudov, R.R. Du, J.A. Simmons, and J.R. Reno, *Phys. Rev. B* **64**, 201311(R) (2001).
2. R. Mani, J.H. Smet, K. von Klitzing, V. Narayanamurti, W.B. Johnson, and V. Umansky, *Nature* **420**, 646 (2002).
3. M.A. Zudov, R.R. Du, L.N. Pfeiffer, and K.W. West, *Phys. Rev. Lett.* **90**, 046807 (2003).
4. A.C. Durst, S. Sachdev, N. Read, and S.M. Girvin, *Phys. Rev. Lett.* **91**, 086803 (2003).
5. V. Ryzhii and R. Suris, *J. Phys.: Condens. Matter* **15**, 6855 (2003).
6. I.A. Dmitriev, M.G. Vavilov, I.L. Aleiner, A.D. Mirlin, and D.G. Polyakov, *Phys. Rev. B* **71**, 115316 (2005).
7. S.A. Mikhailov, *Phys. Rev. B* **83**, 155303 (2011).
8. A.V. Andreev, I.L. Aleiner, and A.J. Millis, *Phys. Rev. Lett.* **91**, 056803 (2003).
9. I.G. Finkler and B.I. Halperin, *Phys. Rev. B* **79**, 085315 (2009).
10. D. Konstantinov and K. Kono, *Phys. Rev. Lett.* **103**, 266808 (2009).
11. D. Konstantinov and K. Kono, *Phys. Rev. Lett.* **105**, 226801 (2010).
12. Yu.P. Monarkha, *Fiz. Nizk. Temp.* **37**, 108 (2011) [*Low Temp. Phys.* **37**, 90 (2011)]; Yu.P. Monarkha, *Fiz. Nizk. Temp.* **37**, 829 (2011) [*Low Temp. Phys.* **37**, 655 (2011)].
13. Yu.P. Monarkha, *Fiz. Nizk. Temp.* **38**, 579 (2012) [*Low Temp. Phys.* **38**, 451 (2012)].
14. D. Konstantinov, Yu.P. Monarkha, and K. Kono, *Phys. Rev. Lett.* **111**, 266802 (2013).
15. D. Konstantinov, A. Chepelianskii, and K. Kono, *J. Phys. Soc. Jpn.* **81**, 093601 (2012).

16. D. Konstantinov, M. Watanabe, and K. Kono, *J. Phys. Soc. Jpn*. **82** 075002 (2013).
17. A.D. Chepelianskii, M. Watanabe, K. Nasyedkin, K. Kono, D. Konstantinov, *Nature Commun*. **6**, 7210 (2015).
18. R.R. Gerhardts, *Surf. Sci.* **58**, 227 (1976).
19. M.I. Dykman and L.S. Khazan, *Zh. Eksp. Teor. Fiz*. **77**, 1488 (1979) [*Sov. Phys. JETP* **50**, 747 (1979)].
20. Yu.P. Monarkha and K. Kono, *Two-Dimensional Coulomb Liquids and Solids*, Springer-Verlag, Berlin (2004).
21. D.B. Mast, A.J. Dahm, and A.L. Fetter, *Phys. Rev. Lett*. **54**, 1706 (1985).
22. D.C. Glattli, E.Y. Andrei, G. Deville, J. Poitrenaud, and F.I.B. Williams, *Phys. Rev. Lett.* **54**, 1710 (1985).
23. P.K.H. Sommerfeld, P.P. Steijaert, P.J.M. Peters, and R.W. van der Heijden, *Phys. Rev. Lett*. **74**, 2559 (1995).
24. S.A. Mikhailov and V.A. Volkov, *J. Phys.: Condens. Matter* **4**, 6523 (1992).